4. NEUTRON AND GAMMA-RAY TOXICITY STUDIES

SUMMARY

E. John Ainsworth, Group Leader

The major program activities are focused in two areas: (1) late effects experiments with large populations of mice which compare the effectiveness of neutron and gamma radiation for production of neoplastic and non-neoplastic diseases and life shortening, and (2) basic studies of cellular and functional indices of radiation injury, which provide the opportunity for fundamental new contributions to the understanding of late radiation effects in the vascular, immune, and hematopoietic systems.

During the past year effort has been devoted to (1) initiation of new late effects experiments with $B6CF_1$ mice to provide a dose-response matrix that will allow the effects of low doses of neutron or gamma radiation, protracted over extended periods of the animals' lifespan, to be precisely measured; and (2) analysis and evaluation of results which are now available from our initial study, JM-2, which began in 1971. Most of the animals in JM-2 are dead and most probable cause of death is being assigned to each animal when analysis of histopathology and/or gross pathology information is completed. The results from JM-2 show a departure from total dose dependence for fractionated doses of both neutron and gamma radiation administered over 24 weeks. When total dose and instantaneous dose rate are held constant and the dose is given in 72, 24, or 6 fractions, the groups that received 6 doses of neutrons showed less life shortening and those that received 6 doses of gamma radiation showed more life shortening than did animals which received 24 or 72 doses. Another departure from additivity observed in neutron-irradiated animals, namely the increase in life shortening and age-specific tumor rate that are produced by dose fractionation, in comparison with the same single dose, is not singularly attributable to induction-promotion of lethal pulmonary tumors, a frequently occurring neoplasm in irradiated $B6CF_1$ mice. The role of age on sensitivity to radiation-induced life shortening produced by a single dose was evaluated in JM-2 and the results show the neutron RBE to be higher at 280 days of age than at 110 days.

Both structural and functional changes in the vasculature have been observed during the second year after irradiation. The structural changes in the pinna include collapse of arteries, arterioles, and some veins along with alterations in the smooth musculature and accumulation of significant fibrosis. Late ultrastructural changes observed in myofibrils involve the endoplasmic reticulum and mitochondria. Other recently initiated work on cardiac muscle also shows alteration in the size and number of mitochondria, and fibrosis

within 75 days after irradiation. The fibrotic reaction, which is especially pronounced in neutron-irradiated animals, indicates a deficiency in repair or proliferative capability. Capillary efficiency, measured by the clearance of subcutaneously injected ^{133}Xe, is influenced by age and by irradiation, and the basis for late qualitative differences in clearance between neutron- and gamma-irradiated animals may become clear when evaluation of structural changes is completed.

Differences in repair or repopulation potential after neutron and gamma radiation are also evident from studies of susceptibility to respiratory infection with *Pasteurella pneumotropica*, and repopulation of splenic lymphocytes which bear the theta antigen. Both end points provide evidence for slower repopulation or restitution of function after a single neutron dose when the dose ratio of gamma to neutron was 2.6. Studies of the age-related decline in cellular immune capability, which provide basic information for the design of other experiments with irradiated animals, show a decrease in the mitogen response of spleen cells cultured *in vitro* which correlates with the previously observed decline in theta antigen.

Studies of early and late injury to the hematopoietic system have continued with particular attention paid to effects of dose fractionation and instantaneous dose rate. The most interesting results concern a sparing effect of low neutron dose rate on repopulation of hematopoietic stem cells (CFU) in the femur, reappearance of circulating platelets, and on the restitution of certain organ weights; however, no dose rate effect on CFU killing, based on D_o, was observed. Thus the effect of neutron dose rate on cell killing and repopulation vary independently in this test system. Since a sparing effect of low neutron dose rate could result from decreased killing of stem cells, measurements of D_o were made for spleen and femur CFU irradiated *in situ*. No differences in D_o were observed at 1.5 and 15 rad/min. This observation is unprecedented. The CFU studies led to experiments which show a significant effect of low neutron dose rate on $LD_{50/30}$ and $LD_{50/7}$.

Work in two areas has been temporarily suspended due to competing activities and/or personnel changes; no reports on transmissible leukemia or radiation effects on microbial systems are presented. The transmissible leukemia was exploited as one model system by which to study the effects of radiation or age on cell-mediated immunity.

Two experiments conducted to evaluate the sensitivity of *Escherichia coli* K12 mutants to JANUS neutrons confirmed and extended the results presented in the 1973 Annual Report. The results show that one mutant which lacks the capacity for both recombination repair and excision repair is markedly sensitive to neutrons. Moreover, since no increase in mutation rate was observed, JANUS neutrons are lethal but not mutagenic in this test system. If funds for continuation of this work are provided, new information will be obtained on the mode of DNA damage produced by neutrons.

During this year, effort has been devoted to several important supportive activities. Preparation for interspecies comparisons which involve the white-footed mouse, *Peromyscus leucopus*, and the beagle are in progress. During the next year, experiments with these species will begin. Our data management systems and data analysis capability which utilize the IBM 370/195 computer are being expanded. Performance of the neutron- and gamma-radiation facilities continues to be excellent, and new hardware procured for gamma

irradiation provides far greater dose rate flexibility than was previously available. In the area of dosimetry, several procedures have been evaluated for calculation of deflection or scatter of gamma rays, and Monte Carlo calculations provide new insight into the influence of radiation configuration or exposure geometry on neutron-gamma dose distribution. Finally, depth dose measurements are reported for a negative pi meson beam produced by the Argonne Zero-Gradient Synchrotron; this study was conducted to evaluate the beam for purposes of biological experimentation.

NEUTRON AND GAMMA-RAY TOXICITY STUDIES STAFF

REGULAR STAFF

Ainsworth, E. John (Biologist)
Allen, Katherine H. (Scientific Associate)
Brennan, Patricia C. (Biologist)
Christian, Emily J. B. (Scientific Associate)
Cooke, Eugenia M. (Scientific Assistant)
Hulesch, Jane L. (Scientific Assistant)
Jordan, Donn L. (Scientific Associate)
Kickels, Wayne T. (Scientific Assistant)
Miller, Marietta (Scientific Associate)
Stearner, S. Phyllis (Biologist)

DOSIMETRY AND DATA MANAGEMENT STAFF

Borak, Thomas B. (Assistant Physicist)
Holmblad, Gordon L. (Scientific Assistant)
Johnson, Emil G. (Engineering Assistant)
Trier, Joseph E. (Engineering Assistant)
Williamson, Frank S. (Physicist)

TEMPORARY STAFF DURING 1974

Yang, Vivian V. (Postdoctoral Appointee)

LATE EFFECTS OF NEUTRON OR GAMMA RADIATION

E. John Ainsworth, R. J. Michael Fry, Frank S. Williamson, Katherine H. Allen, Jane S. Hulesch, Donn L. Jordan, Anthony R. Sallese, and Everett F. Staffeldt

PURPOSE AND METHODS

The objective is to compare the late effects produced by protracted or a single exposure to fission neutrons or ^{60}Co gamma radiation. The information obtained is used to test existing models or develop new models with the aim of predicting (1) any excess risk which results from population exposures to low radiation doses, and (2) the consequences of occupational, therapeutic, or inadvertent exposure to low- or high-LET radiations. The experimental program compares the hazards of low-LET gamma radiation and high-LET neutron

radiation for the induction of late radiation injury, namely neoplastic and non-neoplastic disease, to which excess risk of death is attributable. The principal focus is on determination of dose-response relationships in mice for neoplastic, degenerative, and infectious diseases, and of impairments in physiologic function which occur late in life after low radiation doses administered over long periods of time. Effects of (low) dose rate, dose fractionation, and the portion of the lifespan over which animals are irradiated are evaluated to determine the extent to which estimates of excess risk are dependent on these factors. Any repair or recovery processes operative at low dose rates, or between radiation doses, that serve to diminish late injury are identified.

PROGRESS REPORT

A series of interrelated late effects experiments is currently in progress with $B6CF_1$ mice given either fractionated or single doses of fission neutron or gamma radiation. Results continue to emerge from the first experiment, JM-2, which began in the spring of 1971 (1-5). Most of the animals that received fractionated neutron or gamma doses have died, but many survivors remain among sham-irradiated controls and animals that received low single doses.

Current estimates of mean survival time (MST) after a single radiation dose or the first fractionated dose, administered at ∿ 110 days of age, are shown in Table 4.1. Surviving animals are not included in the MST calculations and groups in which current survival is sufficient to alter the MST estimate are indicated with asterisks. Survival among controls is sufficiently great that the current MST is based on decedents from only the first five replicates which entered the experiment, i.e., half the control sample.

The results in Table 4.1 conform to our previous predictions (2,3), which were based primarily on analysis of results obtained from only three of the ten replicates involved in the experiment, with regard to the following points: (1) under conditions of fractionated exposures administered over 6 months, the neutron RBE for life shortening is ∿ 10, since similar life shortening, ∿ 20%, is produced by 24 weekly doses of 3.3 neutron and 35.7 gamma rad; (2) in the case of single doses, RBE is dose-dependent and is greater than 4.5 at 20 rad and is less than 3.6 at 240 rad; (3) multifractionation of a gamma radiation dose results in a sparing effect on life shortening; the extent of this sparing effect is estimated at approximately threefold, based on days of life shortening per rad and the similar percent life shortening produced by a single dose of 285 rad and the multifractionated doses which total approximately 855 rad; (4) multifractionation of the neutron dose increases, rather than decreases, life shortening; the enhancing effect is statistically significant in both sexes at the total dose of 240 rad and in males that received a total dose of 80 rad.

The mechanism whereby neutron dose fractionation increases life shortening and age-specific tumor rates is not yet clear and is the focus of supporting basic studies reported elsewhere (3). Note that the extent of enhancement is conservatively estimated in Table 4.1 since the MST values are cued from the time of the first fractionated neutron dose.

Table 4.1. Mean Survival Time after Fractionated or Single Doses of Neutron or Gamma Radiation; Experiment JM-2

	Neutron[a]								Gamma[a]							
			Mean Survival Time		Days Lost/Rad		Life Shortening (%)				Mean Survival Time		Days Lost/Rad		Life Shortening (%)	
Group	Total Dose	Fract.[b]	M[c]	F[d]	M	F	M	F	Total Dose	Fract.[b]	M[c]	F[d]	M	F	M	F
A	240	72x3.3	551±13.5	505±11	1.18	1.37	34	39	855	72x11.9	716±12	690±13	0.14	0.17	14	17
B	240	24x10	523±11.5	500±10	1.29	1.39	37	40	855	24x35.7	690±13	676±12	0.17	0.19	17	19
E	240	24x10	545±12	501± 9	1.20	1.38	35	40	855	24x35.7	697±12	694±10	0.16	0.16	16	17
H	240	6x40	575±12	530±10	1.07	1.26	30	36	855	6x143	666±12	642±11	0.20	0.23	20	23
D	80	24x3.3	666±13	675±12	2.1	2. 0	20	19	1140	24x47.5	619±12	612±11	0.19	0.20	26	27
Pooled ABEH		6,24,72	549± 6	510± 5	1.18	1.35	34	39		6,24,72	693± 6	674± 6	0.16	0.19	17	19
S1*	20	1	788±10	761±10	2.2	3.6	5	9		1	806± 9	789± 9	0.28	0.49	3.1	5.2
S2*	80	1	725±13	667±13	1.4	2.1	12	20		1	728±13	704±12	0.39	0.48	12.5	15.5
S3	240	1	633±13	581±13	0.83	1.1	24	30		1	497±15	479±14	0.43	0.45	40.3	42.5
Controls*			832±11 (reps. 1-5)	833±11 (reps 1-5)							832±11 (reps. 1-5)	833±11 (reps. 1-5)				

[a]Based on average absorbed dose/frame.

[b]Number of fractions x dose/fraction; see Table 4.2 for dose rate/fraction.

[c]Males.

[d]Females.

*Several survivors.

Analysis of autopsy and histopathology data and assignment of most probable cause of death permit the conclusion that the enhancing effect of neutron dose fractionation is not solely attributable to lethal pulmonary tumors (LPT), a late-occurring neoplasm observed in approximately 8% of unirradiated control animals and 8-18% of the animals that received fractionated doses of neutron or gamma radiation (Table 4.2). The enhancing effect of neutron dose fractionation is observed both when all causes of death are included in the MST computation, or when animals which died from lethal pulmonary tumors are excluded. The contribution of LPT to survival time is estimated by a decrementation procedure. Results in Table 4.3 show that in unirradiated controls, and in irradiated groups (other than that which received a single dose of 240 rad), when decrementation for LPT was made, the MST was 6-8% longer than in the original sample. The 3% increase in MST produced by decrementation of LPT animals from the group that received the single dose of 240 rad, compared with a 6-7% increase for animals which received fractionated neutron exposures, may indicate: (1) LPT contributes to some extent to the enhancing effect of fractionation; or (2) neutron dose fractionation may decrease the killing of potentially neoplastic cells and thereby permit a greater expression of neoplastic potential than does the same single dose. Comparison of age-specific occurrence rates for LPT in irradiated and unirradiated animals indicates that acceleration of tumor expression is an important component of radiation-induced life shortening. With further analysis of the pathology data, as they become available, it should be possible to evaluate the relative contribution of acceleration-promotion and induction of other neoplasms in irradiated animals.

Table 4.2. Percent Incidence of Lethal Pulmonary Tumors in Irradiated $B6CF_1$ Female Mice

Controls %	Gamma	Dose Rate/ Min	%	Neutron	Dose Rate/ Min	%
	143 rad x 6	0.8	15	40 rad x 6	0.2	16
8	48 rad x 24	1.0	10	3.3 rad x 24	0.07	18
	36 rad x 24	0.8	8	10 rad x 24	0.2	15
	12 rad x 72	0.8	13	3.3 rad x 72	0.2	13
	36 rad x 24	0.1	10	10 rad x 24	0.03	13

Table 4.3. Male $B6CF_1$ Mice Irradiated with Fission Neutrons

Cause of Death	Mean Survival Time (days) Group and Dose				
	Controls[a]	Single Dose 240 rad[b]	Fractionated 240 rad[c]	Single Dose 80 rad[d]	Fractionated 80 rad[e]
All causes	838±13	636±13 [24][g]	553±6 [34]	728±13 [13]	671±13 [20]
All causes other than LPT[f]	906±13 <1.08>[h]	652±13 [28] <1.03>	594±7 [34] <1.07>	768±14 [15] <1.06>	721±13 [20] <1.07>
LPT only	1039±17	919±9	824±8	933±12	879±14

[a] Replicates 1-5.

[b] Replicates 1-10; no survivors.

[c] Replicates 1-10; no survivors.

[d] Replicates 1-10; 12 survivors.

[e] Replicates 1-10; 1 survivor.

[f] LPT = lethal pulmonary tumors.

[g] [ ] % life shortening compared with appropriate control.

[h] < > ratio all causes other than LPT/all causes.

Other new information is now available regarding the additivity of neutron or gamma radiation doses. As detailed above, neutron doses are not simply additive in the sense that fractionation, in comparison with a single dose, increases both life shortening and tumor rates. In addition, the mode of neutron dose fractionation also influences life shortening and thus indicates a second departure from additivity. Significantly less life shortening results in male mice that received 6 doses of 40 rad (1 each 4 weeks) than in animals that received the same total dose, 240 rad, in 24 weekly doses of 10 rad (Table 4.1). The same trend is observed in females.

Although the sparing effect is small, and amounts to a 7% reduction in life shortening in males, the existence of such a phenomenon may indicate either that there is a recovery component which is operative when doses are separated by 4 weeks or that the enhancement is less effectively produced by 6 as compared with 24 or 72 neutron doses. In contrast to the small sparing effect observed when neutron doses are administered in doses separated by 4 weeks, in gamma-irradiated animals this fractionation regimen produces significantly greater life shortening, approximately 6%, than is observed when the same total dose is administered in 72 fractions (3 fractions/week of 12 rad) over 24 weeks (Table 4.1). Since instantaneous dose rate was identical in the 6 and 72 dose groups, the difference in survival time is attributable to dose per fraction or radiation free time. Whatever the mechanism, the results indicate a departure from total dose dependence and identify a recovery component that is operative when the dose per fraction is at a level expected to be on the shoulder of a cell survival curve for gamma radiation.

The matter of comparative susceptibility of male and female mice to radiation-induced life shortening requires further analysis. Significantly shorter survival times are observed among neutron-irradiated females than males in some single and fractionated dose groups. A similar, but not significant, trend is observed among gamma-irradiated mice. Sex-related differences in body weight, which would have a greater effect on dose-distribution in neutron-irradiated animals, may account in part for the apparent sex difference.

Age-susceptibility to life shortening after single doses of neutron or gamma radiation is being evaluated in male mice between the ages of 110 to 278 days. This is the age span over which the fractionated doses in JM-2 were administered. Although several animals remain alive, two interesting trends are clear: (1) irradiation at 194 or 278 days of age causes less life shortening than at 110 days in both neutron- and gamma-irradiated animals; and (2) at 278 days of age, neutrons are more effective than gamma radiation for production of life shortening. When given at 110 days of age, single doses of 80 neutron and 285 gamma rad result in essentially the same MST (725 and 728 days, respectively, or 13% life shortening). When these doses are administered at 278 days of age, the MST after neutron irradiation is significantly shorter than after gamma radiation; thus, life shortening is greater for neutron radiation and age *per se* affords less of a protective effect for neutron than for gamma radiation.

CONCLUSIONS

1. The most probable cause of death has been determined for many of the decedents in JM-2, and it is now possible to evaluate the role of lethal pulmonary tumors in the enhancing effect of fractionated neutron irradiation. Since enhancement is observed when animals with lethal pulmonary tumors are excluded from the data base used for analysis, it is now clear that enhancement is not singularly attributable to promotion or induction of this disease.

2. Departures from total-dose dependence are observed among animals which receive fractionated doses of either neutron or gamma radiation. In the case of neutron radiation, 6 radiation doses produce less life shortening

than do the other dose fractionation protocols (72 or 24 fractions), and in the case of gamma radiation, 6 fractions produce more life shortening than do the other dose protocols. These results identify recovery parameters or departures from simple additivity which are operative under conditions of fractionated neutron or gamma irradiation.

3. Somewhat greater life shortening is observed in irradiated female mice than in male mice. Body size and dose distribution may contribute to this effect.

4. Preliminary results from an experiment designed to evaluate the role of age on sensitivity to radiation-induced life shortening produced by a single dose indicate that the neutron RBE is higher at 278 days of age than at 110 days.

REFERENCES

1. Ainsworth, E. J., R. J. M. Fry, D. Grahn, F. S. Williamson, and J. H. Rust. Proc. Second European Symp. on Late Effects of Radiation (ESLER TWO), Casaccia, Italy, 1972. In press.
2. Ainsworth, E. J., R. J. M. Fry, D. Grahn, F. S. Williamson, and J. H. Rust. Radiat. Res. 55, 531 (1973).
3. Ainsworth, E. J., R. J. M. Fry, D. Grahn, F. S. Williamson, P. C. Brennan, S. P. Stearner, A. V. Carrano, and J. H. Rust. In: Biological Effects of Neutron Irradiation, IAEA, Austria, 1974, p. 359.
4. Ainsworth, E. J., and R. J. M. Fry. Radiat. Res. 59, 314 (1974).
5. Fry, R. J. M., E. J. Ainsworth, E. Staffeldt, A. Sallese, and K. Allen. Radiat. Res. 59, 222 (1974).

EARLY AND LATE INJURY TO THE HEMATOPOIETIC SYSTEM: INFLUENCE OF DOSE RATE AND DOSE FRACTIONATION

E. John Ainsworth, Eugenia M. Cooke, Donn L. Jordan, Jane S. Hulesch, Wayne T. Kickels, and Marietta Miller

PURPOSE AND METHODS

The study of hematopoietic function is important on three counts: (1) the contribution of residual hematopoietic injury to late radiation morbidity and death is unclear; (2) hematopoietic control systems and factors which influence them are fundamental to a disease of considerable interest, leukemia; and (3) the hematopoietic stem cell, evaluated by the spleen colony or colony-forming unit (CFU) technique, offers an excellent model system for studies of injury, repair, proliferation, and subsequent differentiation of stem cell progeny; both the number and functional capability of stem cells can be evaluated independently. The stem cell model has been (1-4) and continues to be exploited in basic studies which focus on an improved understanding of the effects of dose fractionation and dose rate on proliferative tissues. These studies complement the work on life shortening and carcinogenesis (5) and may provide a means by which late effects, such as the

enhanced life shortening produced by fractionated neutron irradiation, may be understood in terms of cellular responses. Methodology utilized in these studies is described elsewhere (6,7).

PROGRESS REPORT

Our previous studies (8) indicated that stem cell repopulation, based on colony-forming units in the femur, occurred earlier in neutron- than in gamma-irradiated animals when the doses given were in proportion to the RBE of 2.6 for 30-day lethality or D_0 for CFU. The advantage observed in neutron-irradiated animals also involved repopulation of peripheral lymphocytes and restitution of spleen weight. This experiment has been repeated, with particular attention to the phase of hematopoietic recovery that occurs between 30 and 180 days after irradiation. The peripheral hematology data are not yet reduced, but the CFU results now available generally confirm our previous observations and indicate that the femur CFU content is higher in neutron-irradiated animals at four sample times between 30 and 60 days. Other new data indicate that the earlier population in neutron-irradiated animals is not attributed to a reduction of the "post-irradiation dip" in femur CFU content in neutron-irradiated animals (9). After single doses of 95 neutron or 247 gamma rad, the dip at 6 hours after exposure is as great, on a percentage basis, in neutron-irradiated as in gamma-irradiated animals and amounts to a 34-36% decline below the femur CFU content at 15 minutes after irradiation. Results from this experiment provide evidence for an earlier onset of femur CFU repopulation in neutron-irradiated mice since by 24 hours the femur CFU content increased significantly compared with the 6-hour content, but in gamma-irradiated animals the femur CFU content did not increase between 6 and 24 hours. When the same total doses of 288 neutron or 744 gamma rad are administered in nine equal fractions over a period of 3 weeks the situation is reversed, compared with the response after a single exposure, and gamma-irradiated animals show an advantage in CFU repopulation. The greater sparing effect of gamma dose fractionation is consistent with expectations and our previous observations which concentrated on the first few weeks after fractionated irradiation (4,10).

We have also repeated our original observation that CFU repopulation is influenced by decreasing the neutron dose rate from 13.1 to 1.5 rad/min (8). Selected data from two experiments are shown in Table 4.4. In both experiments, mice exposed to neutrons at the low dose rate (LDR) of 1.5 rad/min showed a numerical advantage in femur CFU content at some sample times between 12 and 21 days after irradiation. The higher CFU content in animals exposed at the LDR was correlated with higher platelet counts (Table 4.5). Similar sparing effects of low dose rate neutron irradiation are observed at certain sample times for both spleen and thymus weights.

The neutron dose rate effect observed on CFU repopulation presents the requirement to determine if the effect is attributable to a decrease in CFU killing at the LDR or, alternatively, if the effect of neutron dose rate on cell killing and on repopulation varies independently. The effect of neutron dose rate on D_0 for CFU has been determined by irradiating donor animals with the test dose, sacrificing the animals, and measuring the number of surviving CFU. With this experimental design the CFU are irradiated *in situ* rather than after they have been sequestered in the spleen following intravenous

Table 4.4. Colony-Forming Units (CFU) in the Femur after 288 Rad of Neutron Radiation Administered at 13.1 (HDR) or 1.5 (LDR) Rad/Min. At Each Sample Time Marrow from 2 to 4 Donors was Pooled and Injected into 15 to 20 Recipient Animals

Days after Irradiation	Means and 95% Confidence Limits			
	High Dose Rate (HDR)		Low Dose Rate (LDR)	
	Experiment 2	Experiment 3	Experiment 2	Experiment 3
0	6152 (5248-7057)	7345 (6599-8090)	-	-
12	464 (391-538)	583 (511-654)	653 (564-743)[a]	519 (428-609)
14	784 (615-954)	810 (655-954)	1246 (1047-1446)[a]	1460 (1210-1710)[a]
16	821 (671-972)	927 (794-1059)	1839 (1439-2240)[a]	1580 (1385-1776)[a]
18	1695 (1352-2038)	1145 (924-1366)	2602 (2086-3118)[a]	1440 (1192-1688)
21	1369 (1119-1619)	-	2376 (2019-2733)[a]	-

[a]Significantly higher than HDR at the .05 level.

Table 4.5. Platelet Counts in Peripheral Blood after 288 Rad of Neutron Radiation Administered at 13.1 (HDR) or 1.5 (LDR) Rad/Min. Group Sizes in Experiments 2 and 3 were 15 and 20 per Sample Time, Respectively

Days after Irradiation	Means and 95% Confidence Limits			
	High Dose Rate (HDR)		Low Dose Rate (LDR)	
	Experiment 2	Experiment 3	Experiment 2	Experiment 3
0	1325 (1236-1414)[a]	1365 (1345-1491)[a]	1334 (1250-1419)[a]	1368 (1293-1443)[a]
12	109 (92-127)	96 (81-111)	198 (160-236)	168 (145-191)
14	232 (198-265)	191 (163-220)	339 (297-382)	343 (314-371)
16	422 (373-510)[b]	340 (313-367)	556 (461-651)	570 (504-636)
18	632 (526-738)	522 (471-573)	867 (758-977)	843 (773-912)
21	884 (803-965)[b]	-	980 (908-1051)	-

[a]Four separate control groups, which totalled 65 animals, were evaluated.

[b]Difference between HDR and LDR is not significant; all other differences within Experiments 2 and 3 are significant ($P < 0.05$).

injection of marrow. The results available at this time indicate no significant effect of neutron dose rate on D_o for femur or spleen CFU. The current estimates are 39 ± 4 and 41 ± 1.3 rad for femur CFU and 31 ± 1 and 31 ± 1 rad for spleen CFU irradiated at low and high dose rates, respectively. The absence of a dose rate effect for fission neutrons from JANUS on CFU survival is consistent with earlier observations by Sinclair with Chinese hamster cells *in vitro*, who found no effect of dose rate on D_o (11).

Since injury to the hematopoietic system contributes significantly to neutron lethality in the $LD_{50/30}$ dose range, the higher CFU content in animals exposed at the LDR would predict some sparing effect or increase in $LD_{50/30}$ at 1.5 rad/min providing femur CFU content is correlated with survival and if the acceleration of recovery occurs at a sufficiently early time to benefit the irradiated animal. The results in Table 4.6 show a small, ∿ 7%, reproducible, and statistically significant increase in $LD_{50/30}$ at the LDR. In the experiment dated 9/74, confinement stress was controlled by retaining the animals exposed at the high dose rate (HDR) of 13.1 rad/min in the containers in which they were irradiated for the maximum period of confinement required to deliver the highest dose given at the LDR, e.g. ∿ 6 hrs. Since confinement stress produced no detectable effect on $LD_{50/30}$ at the high dose rate, the inference is that the 7% increase in $LD_{50/30}$ is specifically attributable to the decrease in dose rate. The results in Table 4.6 show that both $LD_{50/6}$ and $LD_{50/7}$ are increased at the LDR, and the percentage increase, 13%, is relatively greater than is observed for $LD_{50/30}$. This conforms to general expectations regarding repair capacities of hematopoietic and intestinal stem cells, respectively. The increase in $LD_{50/7}$ at the LDR is statistically significant and the change in $LD_{50/6}$ is borderline.

Table 4.6. Effect of Neutron Dose Rate on 6-, 7-, and 30-Day Mortality in $B6CF_1$ Male Mice

End Point	Dose Rate (rad/min)	LD_{50}(rad) and 95% Confidence Limits — Individual Determinations		Pooled LD_{50} Estimate
6-Day Lethality	1.5	4/74 678 (569-792) 9/74 638 (595-682)		662 (608-717)
	15	1/73 565 (395-737) 4/74 606 (575-637)	4/73 545 (510-581) 9/74 612 (578-647)	586 (561-611)
7-Day Lethality	1.5	4/74 628 (556-699)	9/74 616 (585-648)	626 (591-662)
	15	1/73 559 (509-609) 4/74 562 (516-609)	4/73 497 (456-540) 9/74 580 (554-607)	553 (541-567)
30-Day Lethality	1.5	8/73 479 (461-498) 9/74 475 (462-490)	1/74 465 (458-474)	474 (469-478)
	15	1/73 456 (442-471) 4/74 442 (410-435)	12/73 442 (425-459) 9/74 445 (438-453)	443 (437-451)

These results which show a significant effect of neutron dose rate on $LD_{50/30}$ are at variance with earlier reports by Vogel et al. (12), and a more recent report by Gottlieb and Gengozian (13). Although fission spectrum neutrons were used in the present experiments as well as those cited above, spectral differences as well as the use of different mouse strains may contribute to the differences between the present and the earlier observations. Since the gamma radiation component of the total dose sustained by animals exposed in the JANUS reactor facility is lower than the gamma component encountered in other exposure facilities, including those cited above,

difference in the amount of low-LET radiation in the radiation fields cannot account for the difference between the present and earlier observations. This matter requires further consideration and must be viewed with full cognizance of the fact that not all of the dose deposited by recoil protons, produced by neutron interactions in hydrogenous matter, is densely ionizing.

Other continuing studies of the hematopoietic system concentrate on functional studies that reveal late-occurring deficiencies which are not necessarily correlated with low peripheral blood counts or reductions in the size of the stem cell compartment. We previously reported (1) that by 280 days after 288 neutron or 741 gamma rad the femur and spleen stem cell content in irradiated animals did not differ significantly from aged unirradiated controls, but that the irradiated animals showed a significantly reduced ability to respond to bacterial endotoxin with CFU proliferation in the marrow or spleen. These results were confirmed in a replicate experiment. An experiment conducted at 350 days after fractionated doses of neutron or gamma radiation (total doses of 288 neutron or 741 gamma rad given in 9 equal doses over 21 days) shows generally similar phenomenology (Table 4.7). A difference between these and the previous observations after a single irradiation concerns the femur and spleen CFU content of animals before endotoxin injection. Femur CFU content in the animals that received fractionated neutron or gamma irradiation was significantly lower than in aged controls. This could indicate incomplete repopulation, or an accelerated decline in the stem cell population, both of which we have observed previously (1). Moreover, the endotoxin response in irradiated animals, reflected by reduced rather than increased CFU content, differs significantly from the response of aged controls between 3 and 5 days after injection. In irradiated survivors, both neutron- and gamma-irradiated, endotoxin produced a significant decline in femur CFU content which occurred more rapidly and to a lower level than in aged controls. The spleen response was similar to that observed at 280 days after a single irradiation; namely, some delay in the increase in CFU content in irradiated animals. The basis for these differences in proliferative response to endotoxin, which constitute some mode of residual injury, is unknown at this time, but results of Roy Vigneulle,* a graduate student in our laboratory, show that the late lesion may not reside with the stem cell *per se*. His work shows that the proliferation rate, e.g. doubling time, of stem cells from aged irradiated survivors and aged animals, after transplantation into young supralethally-irradiated recipients, does not differ significantly, although the femur content of CFU from the original irradiated donor animals was reduced in comparison with aged controls. Thus, late injury to "control systems" or stroma, rather than a component of injury to CFU *per se* may account for these results. Experiments designed to test that hypothesis are planned.

*Laboratory Graduate Program Participant, University of Illinois, Urbana.

Table 4.7. Femur and Spleen Content of Colony-Forming Units (CFU) in $B6CF_1$ Mice Injected with 0.1 ml Typhoid Vaccine at Approximately 350 Days after Irradiation[a]

Days after Injection	Organ	Aged Controls	Neutron	Gamma
1	Bone Marrow	5179 (4049-6308)	5700 (4485-6915)	4167 (3091-5243)
	Spleen	2383 (1840-2927)	2300 (1877-2723)	2288 (1792-2785)
2	Bone Marrow	5066 (3655-6478)	3653 (2778-4529)	3666 (2187-5146)
	Spleen	5600 (4668-6532)	3813 (3259-4368)[b]	4615 (3349-5882)
3	Bone Marrow	6143 (4745-7541)	3700 (2871-4529)[b]	2167 (1437-2897)[b]
	Spleen	5627 (4468-6785)	6213 (5003-7426)	5200 (4132-6268)
4	Bone Marrow	5333 (4382-6285)	2733 (2089-3377)[b]	3153 (2389-3918)[b]
	Spleen	5464 (4141-6787)	4800 (3740-5860)	4420 (3729-5110)
5	Bone Marrow	4321 (3163-5479)	3071 (2153-3990)	2808 (2013-3603)
	Spleen	4343 (3549-5137)	4027 (3213-4840)	2400 (1610-3190)[b]
No Injection[c]	Bone Marrow	7071 (5934-8208)	4500 (3201-5799)[b]	4692 (3493-5892)[b]
	Spleen	2900 (2332-3468)	3883 (3330-4437)	1468 (1222-1714)[b]

[a]The fractionated irradiation schedule consisted of 9 doses of 10.7 neutron rad or 27.4 gamma rad administered over 3 weeks. The dose rates were 0.6 and 1.5 rad/min for neutron and gamma radiation, respectively. Total doses were 96 neutron and 247 gamma rad. The first radiation fraction was administered at 110-120 days of age.

[b]Significantly different from aged controls.

[c]460-470 days of age.

REFERENCES

1. Ainsworth, E. J., R. J. M. Fry, D. Grahn, F. S. Williamson, and J. H. Rust. Proc. Second European Symp. on Late Effects of Radiation (ESLER TWO), Casaccia, Italy, 1972. In press.
2. Ainsworth, E. J., R. J. M. Fry, D. Grahn, F. S. Williamson, and J. H. Rust. Radiat. Res. 55, 531 (1973).
3. Ainsworth, E. J., R. J. M. Fry, D. Grahn, F. S. Williamson, P. C. Brennan, S. P. Stearner, A. V. Carrano, and J. H. Rust. In: Biological Effects of Neutron Irradiation, IAEA, Vienna, 1974, p. 359.
4. Ainsworth, E. J., and R. J. M. Fry. Radiat. Res. 59, 314 (1974).
5. Ainsworth, E. J., R. J. M. Fry, F. S. Williamson, K. H. Allen, J. S. Hulesch, D. L. Jordan, A. R. Sallese, and E. F. Staffeldt. Late effects of neutron or gamma radiation. This Report, Section 4.
6. Ainsworth, E. J., and R. M. Larsen. Radiat. Res. 40, 149 (1969).
7. Ainsworth, E. J., R. J. M. Fry, D. Grahn, F. S. Williamson, J. H. Rust, P. C. Brennan, A. V. Carrano, D. L. Jordan, M. Miller, K. H. Allen, M. P. Nielsen, E. Cooke, E. Staffeldt, and A. Sallese. ANL-7970 (1972), p. 13.
8. Miller, M., E. Cooke, and E. J. Ainsworth. Radiat. Res. 51, 473 (1972).
9. Broerse, J. J. Curr. Top. Radiat. Res. Q. 8, 305 (1973).
10. Ainsworth, E. J., R. J. M. Fry, F. S. Williamson, W. E. Kisieleski, D. L. Jordan, M. P. O'Malley, M. Miller, E. M. Cooke, A. Sallese, and P. C. Brennan. ANL-7870 (1971), p. 19.
11. Sinclair, W. K. ANL-7770 (1970), p. 29.
12. Vogel, H. H., Jr., J. W. Clark, and D. L. Jordan. Radiat. Res. 6, 460 (1957).
13. Gottlieb, C. F., and N. Cengozian. J. Immunol. 109, 711 (1972).

STRUCTURAL CHANGES IN THE MICROVASCULATURE IN THE AGING, IRRADIATED MOUSE

S. Phyllis Stearner, Rosemarie L. Devine, and Emily J. B. Christian

PURPOSE AND METHODS

Damage to small blood vessels is frequently associated with injury from radiation, from other environmental pollutants, and also from normal aging. Serious vascular damage may be produced by radiotherapy in tissues near the tumor or surrounding it. This injury can endanger the patient even when the tumor has been successfully treated. Heart failure, for example, is recognized as a potential hazard months or years after irradiation of the heart during treatment of tumors of breast or lung.

Long-term studies of the vascular effects of low-level radiation exposures are in progress as part of the JANUS Program. These studies include direct microscopic observations of the circulation in the mouse pinna, estimations of capillary efficiency (i.e., capillary blood flow) in selected tissues, and ultrastructural observations of the microvasculature. Observations are scheduled at approximately 6-month intervals. Longitudinal studies over the lifespan of individual animals will make possible comparisons of vascular changes with radiation treatment and with the effects of fractionation. The most characteristic effects, observed *in vivo* with the light microscope, include constriction or segmental stenosis of arterioles and dilatations or tortuosities of venules. Our study of ultrastructural changes, correlated with *in vivo* observations, includes evaluation of the radiation effects that occur at approximately the time of maximum decrease in the circulatory efficiency, at about 18 months. These observations are preliminary and only tentative correlations can be made with radiation treatments at this time.

Direct microscopic observations of the vasculature in the mouse pinna were recorded photographically on 35-mm film and 16-mm movie film strips for later comparative evaluations. Selected individuals were sacrificed at about 24 months of age for fine-structural study of specific regions of the pinna that *in vivo* studies had previously identified to be of special interest. The radiation dose groups from which electron microscopic studies are reported include fission neutron exposures to 240 rad, the same neutron dose fractionated over a 24-week period, ^{60}Co gamma rays (85[illegible] rad) also delivered over 24 weeks, and unirradiated controls. Details of procedures have been described (1).

RESULTS

The major artery in the pinna should probably be classified as an arteriole. It contained at least one complete elastic layer, a layer of smooth muscle of varying thickness, and a continuous endothelium. At higher magnifications, electron-microscope observations showed that the elastic lamina has a homogeneous and rather uniform appearance. Smooth muscle cells had few dilated vacuoles, and in general appeared to undergo little alteration with age. The major venule of the pinna, which parallels the arteriole, was composed of a layer of continuous endothelium, some collagen fibers outside the basement membrane, and a more or less continuous layer of smooth muscle.

The components of capillaries, present in varying abundance in different regions of the pinna, included a continuous endothelium, a thin basement lamina surrounding the endothelium, and an occasional adjacent pericyte.

After a single exposure to 240 rad fission neutrons, marked ultrastructural effects on arterioles and venules were seen in animals sacrificed about 20 months after exposure. Arterioles were frequently completely collapsed, the lumen barely discernible. The endothelium appeared continuous (no open junctions or breaks), but the surrounding elastica was markedly changed. Instead of having a homogeneous appearance, the elastica contained myelin figures and regions of fibrosis. In general, thicker layers of collagen were present around both types of vessels. Venules also tended to be collapsed and the muscle layer was frequently discontinuous. The venular endothelium was intact, but showed a variety of changes. Frequently, electron-lucent cells were present adjacent to electron-dense endothelium. The endothelium was surrounded by an increased amount of basement lamina material.

In groups that received fractionated neutron doses, segmental arterial stenosis was especially prominent, marked ultrastructurally by regions of extensive fibrosis in the smooth muscle layer. Frequently myofibrils were completely replaced by fibers presumably collagenous in nature. There were also numberous vacuoles, dilated endoplasmic reticulum, and degenerated mitochondria. Endothelium was frequently irregular. The elastica contained vacuoles, fibrillar material, and myelin figures, all of which represented marked changes from the normal homogeneous appearance. The larger venules contained a disordered array of collagen fibers and only occasional bits of smooth muscle. Generally, the endothelium was continuous with little indication of irregularities.

In contrast to the extensive vascular change in neutron-irradiated animals, fractionated exposures to 855 rad of ^{60}Co gamma radiation resulted in less prominent alterations. Arterioles from comparable regions of the pinna showed few changes; the endothelium was intact, smooth muscle layers were complete, and only minimal alterations were present in the elastic lamina. The large, thin-walled venules adjacent to the arterioles, however, sometimes showed discontinuous endothelium, partial atrophy or disappearance of the muscle layer, and increased collagen accumulation. Capillaries tended to be swollen, with enlarged endothelial vacuoles that frequently occluded the lumen. Thickened basement laminae were again prominent. Of special interest was the appearance of endothelial proliferation in arteries. The resulting projections contained significant amounts of elastic material in addition to endothelium and led to obstruction of blood flow in effected vessels. There was also an unusual amount of pinocytosis.

CONCLUSION

In neutron-irradiated animals, fibrosis was much more notable than in gamma-irradiated animals and there was apparently less cell proliferation for injury repair. Segmental stenosis, a characteristic late radiation effect, most prominent after neutron radiations, appeared to be a consequence of smooth muscle changes. Smooth muscle degeneration and fibrosis appeared to be more marked after fractionated than after single neutron exposures.

Development of irregularly dilated venous segments, associated with aging as well as radiation damage, appeared to be the result of degeneration of the smooth muscle of the vessel wall. Capillaries were frequently occluded by swollen endothelium.

REFERENCE

1. Stearner, S. P., and R. L. Devine. ANL-8070 (1973), p. 22.

FINE STRUCTURE OF THE IRRADIATED HEART

S. Phyllis Stearner and Vivian V. Yang

PURPOSE AND METHODS

Radiation effects on the heart are recognized as a possible cause of complications associated with various procedures in radiotherapy. Some years ago, Kohn et al. described changes in the mouse heart a year or more after exposure to whole-body X-radiation (1). In general, however, this organ is considered to be fairly radioresistant and has received little attention in studies of radiation effects of relatively low-level total-body exposures. Observations in the chicken (2) indicated that late appearance of myocardial atrophy and pericardial fibrosis frequently resulted from whole-body exposures to ^{60}Co gamma radiations at or near the acute lethal range. In addition, rabbits and mice showed histological evidence of myocardial damage after partial-body exposures to 1000 or 2000 rad X-radiation (3-5). In connection with long-term observations of gamma and fission neutron effects in the JANUS Program, studies are in progress to determine ultrastructural changes in the myocardium and myocardial microvasculature associated with age and with radiation treatment. These changes will be compared with vascular effects in the pinna.

The animals in this study received a single, total-body dose of 240 neutron rad, or 285 or 855 gamma rad, or were unirradiated controls. Animals were sacrificed by ether inhalation at 4, 30, 75, and 180 days after irradiation. The thorax was opened, and the heart was perfused through the left ventricle with Karnofsky's paraformaldehyde-glutaraldehyde fixative, pH 7.4. After perfusion, cross-sections of the major vessels (aorta and inferior vena cava) were removed. The heart was sectioned below the auricles, perpendicular to the long axis, and blocks of tissue were taken from the left and right ventricles, using a constant sampling site in all animals. All specimens were fixed in fresh Karnofsky's fixative for 3 to 5 hours at 4°C. After overnight wash in buffer, tissues were post-fixed with osmium tetraoxide, dehydrated in alcohol, stained *en bloc* with uranyl acetate in 75% alcohol, and embedded in Epon-Araldite mixture. Survey sections cut at 1-μm thickness and stained with toluidine blue were prepared for light microscopy. Thin sections were examined and photographed in the Siemens electron microscope.

RESULTS

Ultrastructural changes in cardiac muscle were seen at 4 days after irradiation. Myocardial cells showed fibrillar disorganization, accumulation of myelin figures, and lysosomal-like bodies. Z-lines and mitochondria were generally unchanged. At 75 days, fibrillar degeneration was more advanced, with loss of entire myofibrils. Many of these areas contained double-membrane vesicles, electron-dense debris, dispersed ribosomes, and partially vacuolated mitochondria. In some myofibrils, Z-bands showed total destruction. Some muscle fibers had disrupted intercalated disks. Interstitial fibrosis surrounding the muscle fibers was also observed at 75 days. There appeared to be slightly greater injury in the neutron-irradiated than in the gamma-irradiated animals. At 4 and 75 days post-irradiation, the myocardial capillaries also showed a variety of ultrastructural changes. Endothelial cell swelling varied from capillary to capillary and in some instances was also markedly different in adjacent endothelial cells. In addition to swelling, endothelial cells also showed extensions and blebbing, myelin-like figures, and vacuolated mitochondria. Thrombi were frequently observed adhering to irregularities of the endothelial surface.

Only preliminary observations of other treatment groups have been completed. It is anticipated that quantitative evaluations can be made of the extent of myofibrillar degeneration and of capillary abnormalities. Changes in the size and number of mitochondria in the muscle fibers, suggested by preliminary evaluations, will receive further study.

REFERENCES

1. Kohn, H. I., R. F. Kallman, C. C. Berdjis, and K. B. DeOme. Radiat. Res. 7, 407 (1957).
2. Stearner, S. P., and E. J. B. Christian. Radiat. Res. 52, 179 (1972).
3. Fajardo, L. F., and J. R. Stewart. Lab. Invest. 29, 244 (1973).
4. Khan, M. Y. Am. J. Pathol. 73, 133 (1973).
5. Khan, M. Y., and M. Ohanian. Am. J. Pathol. 74, 125 (1974).

RADIATION EFFECTS ON CIRCULATORY EFFICIENCY

S. Phyllis Stearner and Emily J. B. Christian

PURPOSE AND METHODS

Studies of alterations in circulatory function in the mouse have been carried out in connection with studies of structural changes in the vasculature resulting from radiation exposures and from natural aging (1). The clearance of locally administered radioactive xenon, Xenon-133, is a rapid and non-destructive method for determination of capillary blood flow in specific tissue regions. It can be carried out conveniently in the mouse. Radioactive xenon in saline solution is injected into a subcutaneous tissue region, from which it enters the circulating blood through the capillary

endothelium. It is then removed from the region by means of venous outflow to the lungs where about 95% of the injected amount is expired in the first circulation.

The amount of injected ^{133}Xe for each determination was about 0.02 ml containing 50 to 100 μCi. A Packard 400-channel analyzer equipped with a sodium iodide crystal was used to count the 80 keV gamma ray emitted. The entire mouse was monitored at a position 21 cm from the face of the crystal to determine the loss from the subcutaneous region. Counting was continuous for more than 30 minutes during injection and the subsequent washout period. The time per channel was 5 seconds. The dose groups for which mean clearance values are reported here include single doses of 240, 80, and 20 rad of fission neutrons, and 855 and 285 rad of ^{60}Co gamma rays. Additional dose groups will be reported later.

RESULTS

Clearance of locally injected radio-xenon from a subcutaneous region was usually adequately fitted by a single exponential in both controls and irradiated mice. The mean half time was approximately 10 minutes in unirradiated controls, up to about 20 months of age.

The effect of irradiation and of age on capillary efficiency are shown in Figures 4.1 and 4.2. In controls from 24 to 30 months, the circulatory efficiency decreased, as indicated by an increase in half time of xenon clearance to 13 to 14 minutes from the earlier level of 10 minutes. After this, however, when group mortality exceeded 50%, there was an increase in capillary efficiency as a preterminal condition was reached. In the various irradiated groups, capillary efficiency also tended to increase at approximately the time at which group mortality had exceeded 50%. In individuals nearing a terminal state clearance was frequently even more rapid than in young controls. Following a neutron dose of 240 rad, there was an early increase in capillary efficiency and at 3 days after exposure mean clearance half time was only about 5 minutes. At 4 days, however, the mean values returned to the control level and remained at this level through 30 days. After some months, clearance in the neutron-exposed groups tended to be only slightly slower than in controls and there was no clear dose-dependence. All groups showed a preterminal increase in capillary efficiency (faster clearance) that paralleled the control response. After a ^{60}Co gamma dose of 855 rad, there was an early increase in capillary efficiency that was sustained through 7 days. Clearance was much slower than in controls during the 3- to 12-month period after gamma irradiation. Again there was no clear dose-dependence. A preterminal increase in clearance time, corresponding to the time of increased mortality, was observed as in the control and neutron-irradiated groups.

CONCLUSIONS

Clearance times of subcutaneously injected Xenon-133 generally increased with age in all irradiated groups and, to a lesser degree, in controls. There was a more rapid clearance in neutron- than in gamma-irradiated groups that suggested a qualitatively different change was operative in these groups.

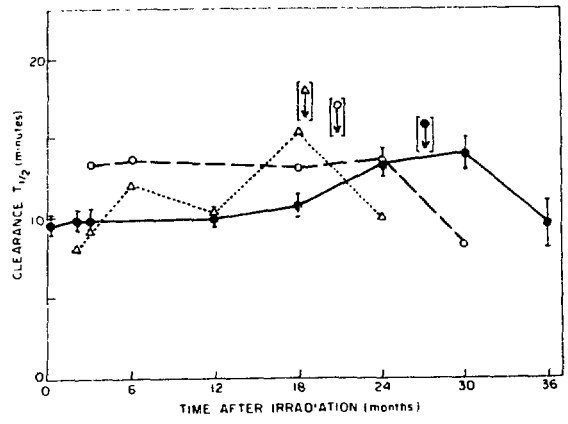

Fig. 4.1. Effect of single-dose, total-body irradiation with fission neutrons on capillary efficiency, indicated by the half time ($T_{1/2}$) of ^{133}Xe clearance from the subcutaneous region in the mouse. Arrows indicate the time at which mortality reached 50% in each of the treatment groups. Error bars represent 1 SE.
- ● Control
- o 80 rad
- Δ 240 rad

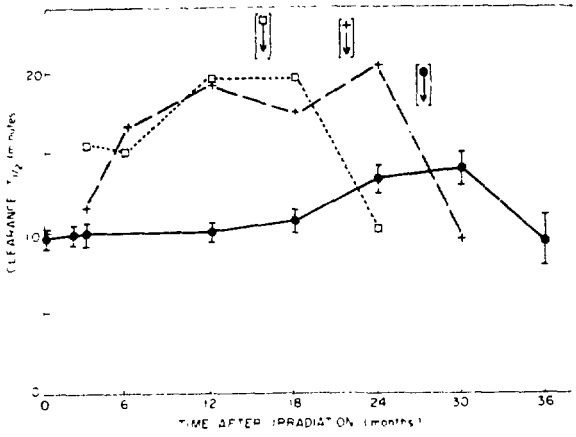

Fig. 4.2. Effect of single-dose, total-body irradiation with ^{60}Co γ-rays on capillary efficiency, indicated by the half time ($T_{1/2}$) of ^{133}Xe clearance from the subcutaneous region in the mouse. Arrows indicate the time at which mortality reached 50% in each of the treatment groups. Error bars represent 1 SE.
- ● Control
- \+ 285 rad
- □ 855 rad

A contributing factor to decrease in capillary efficiency (that is, the longer clearance time) may be the fibrosis that is commonly observed after radiation (1). A more efficient circulation in the preterminal period is not a unique response associated with irradiation, but is also seen in unirradiated controls.

Interpretation of factors influencing changes in capillary efficiency in irradiated mice will require information from related studies ongoing in the JANUS Program. Correlation with structural findings will be of value.

REFERENCE

1. Stearner, S. P., R. L. Devine, and E. J. B. Christian. Structural changes in the microvasculature in the aging, irradiated mouse. This Report, Section 4.

RADIATION EFFECTS ON HOST DEFENSE MECHANISMS

*Patricia C. Brennan, Wayne T. Kickels, Richard C. Simkins, and Linda G. Daniel**

PURPOSE AND METHODS

Resistance to disease depends as much on the integrity of host defense mechanisms as on the invasive and/or toxic properties of the disease-producing agent. The ability to mount an adequate cellular defense may determine the outcome of exposure to certain viral, bacterial, and mycotic infections. Similarly, cellular immune competence is believed to influence tumor cell proliferation as well as forming the surveillance system that eliminates tumor cells when they arise spontaneously. Resistance to other diseases may depend more on the ability of specialized host cells to phagocytize and kill the invading microorganism, to mount a humoral response, or to produce interferon. Any injury which impairs one or more of the many interacting host defense mechanisms can upset the delicate balance that exists between health and disease.

While it is well known that increased susceptibility to infectious disease, and hence impaired host defense, follows acute mid-lethal exposure to low-LET radiation, little is known about the effect on host defense of chronic low-level exposure or about either acute or chronic exposure to high-LET radiation.

We are assessing the integrity of host defense mechanisms of the irradiated $B6CF_1$ mouse by determining: (1) the functional state of the pulmonary antibacterial system, measured by clearance of *Pasteurella pneumotropica;* (2) the ability to mount a cellular and humoral response to challenge with *Mycoplasma pulmonis*; (3) cellular immune competence by spleen thymus-derived (T) cell content and response to T-cell mitogens; (4) humoral immune competence by response to the B-cell mitogen, bacterial lipopolysaccharide (LPS). Experiments have also been initiated to study cellular immune competence in *Peromyscus leucopus* and the beagle dog (see Section 2, Radiation Toxicity in Dogs). With the exception of the *in vitro* response to mitogens, details of the methods have been previously reported (1-4).

The response of cultured spleen cells to mitogens is determined by measuring the incorporation of tritiated thymidine into DNA after 72 hours culture with optimum doses of the T-cell mitogens, Concanavalin A (Con A) and Phytohemagglutinin (PHA), and the B-cell mitogen LPS.

PROGRESS REPORT

Table 4.8 shows the clearance of *P. pneumotropica* from the lungs of mice 5, 11, and 21 days after single doses of 288 neutron rad or 740 gamma rad. Little repair is evident in neutron-irradiated mice; 85% were unable to clear the organism when challenged as long as 21 days after irradiation, whereas only 25% of gamma-irradiated mice failed to eliminate *P. pneumotropica*.

---

*Summer 1974 participant in the Undergraduate Honors Research Participation Program, Clark College.

Table 4.8. Clearance of *Pasteurella pneumotropica* from the Lungs of Neutron- or Gamma-Irradiated Mice

Time of Challenge[a]	Radiation Dose (rad)[b]	Viable *P. pneumotropica* Recovered/Lung (10^2)[c]	Percentage of Mice Unable to Clear *P. pneumotropica*
5 days	fn 288	29.0 ± 12.2	70.4
	γ 740	4.2 ± 2.2	72.0
11 days	fn 288	280.0 ± 83.0	93.1
	γ 740	5.1 ± 1.8	66.0
21 days	fn 288	38.0 ± 13.0	85.2
	γ 740	0.27 ± 0.09	25.0
5-21 days	0	0.05 ± 0.005	7.3

[a]Groups of 30 mice were challenged with 3×10^5 viable *P. pneumotropica* and their lungs cultured 4 days later.

[b]Factors used to convert exposures to midline tissue dose were 0.80 for JANUS neutrons and 0.95 for ^{60}Co gamma radiation.

[c]Values are the mean ± 1 SE.

These data suggest an RBE of > 2.6 for this end point. Immunofluorescent-stained lung sections at all time intervals were strikingly similar among neutron- and gamma-irradiated and unirradiated mice. Alveolar macrophages were swollen with fluorescent *P. pneumotropica* cells and macrophages surrounding the bronchi and in the bronchial exudate were also intensely fluorescent. The immunofluorescence data coupled with the culture data indicate that while pulmonary macrophages in the irradiated host are capable of engulfing invading *P. pneumotropica* cells, the ability to kill them is impaired.

We have continued our efforts to develop more sensitive tests for the detection of antibody to *M. pulmonis*. A radioimmunoprecipitation (RIP) test has been developed which is more sensitive than the mycoplasmacidal test we reported previously (4). The RIP test has the added advantage that levels of different immunoglobulin classes can be determined. We are presently determining the level of anti *M. pulmonis* IgG in the serum and anti *M. pulmonis* IgA in nasal washings of experimentally infected mice.

During this reporting period, we have completed a study of the early changes in T-cell spleen populations following neutron or gamma irradiation. Results 5, 11, and 21 days after single doses of 288 neutron or 740 gamma rad are shown in Figure 4.3. In gamma-irradiated mice, the T-cell content is depressed by 70% at 5 days, but returns to normal by 21 days. In neutron-irradiated animals, the T-cell content is depressed by 82% 5 days after

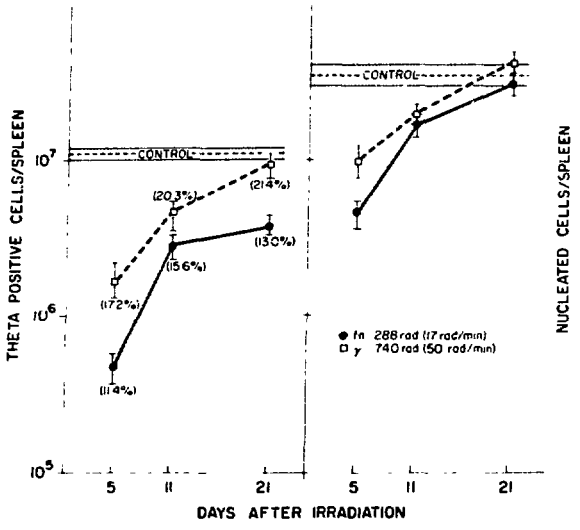

Fig. 4.3. The effect of irradiation on the spleen T-cell content and on total spleen cellularity 5, 11, and 21 days after irradiation, with the associated standard error. The percentage of T cells is shown in parentheses.

irradiation and by 21 days is still 20% below normal, although the total spleen cellularity has returned to normal. An experiment to determine the T-cell content at later times after a single dose of 240 neutron or 855 gamma rad is in progress. Eight to 10 weeks after irradiation the T-cell content in gamma-irradiated mice is depressed by 33%, whereas that in neutron-irradiated mice is depressed by 42%. Twenty, 36, and 44 weeks after neutron irradiation the spleen T-cell content is depressed by $\sim$ 30%, whereas 20 weeks after gamma irradiation the T-cell content is only depressed 18%. Data from later time periods after gamma irradiation are incomplete. We have examined some selected single-dose mice from the JM-2 experiment 78 to 116 weeks after irradiation. The T-cell content in gamma-irradiated mice is not significantly different from that in control mice, whereas that of neutron-irradiated mice is $\sim$ 50% that of comparably aged controls. These data suggest an RBE of > 3.6 at these later time points.

Since our future plans involve interspecies comparisons with *P. leucopus*, we have determined that *P. leucopus* T cells carry the θ AKR allele, in contrast to $B6CF_1$ mouse T cells which carry the θ C_3H allele. High titer anti θ AKR serum has been prepared which will allow us to compare the spleen T-cell content of irradiated *P. leucopus* with that of $B6CF_1$ mice.

Studies on the response of cultured mouse spleen cells to mitogens have been initiated during this reporting period. Preliminary experiments were designed to determine the optimum culture conditions and the mitogen concentration that gives maximum stimulation. We have found that culture of 1.5×10^6 viable nucleated spleen cells in RPMI 1640 medium supplemented with 2 mM glutamine, 10% heat-inactivated fetal calf serum, and 100 μg/ml of penicillin and streptomycin for 72 hours is optimal. The cells are suspended in 0.9 ml medium, and mitogen diluted in 0.1 ml medium is added at 0 time. The cultures are then incubated for 48 hours at 37°C in 5% CO_2. They are then pulsed with 1 μCi of tritiated thymidine (specific activity, 6 Ci/mM) and re-incubated for 18 hours. The cells are collected on Millipore filters, and the DNA precipitated with cold TCA. After drying, the filters are counted

in a liquid scintillation counter. We have found that the final concentration of Con A and PHA that gives maximum stimulation is 2 μg/ml. For LPS (Piromen, Flint Laboratory) the dose is 0.2 μg/ml. Table 4.9 shows preliminary data on the age and radiation related response of cultured spleen cells to mitogen stimulation. There is a significant decline in the response to Con A and PHA between 160 and 415 days of age. This decline parallels our previously reported decline in theta antigen with age (3). A similar decline is inferred in the response to the B-cell mitogen LPS from comparison of the tritiated thymidine activity of cells from 100-day-old mice and from 415-day-old mice. There was no significant difference to mitogen stimulation between irradiated and unirradiated control animals 250 days after gamma irradiation, or 415 days after neutron irradiation; however, the sample sizes were very small.

Table 4.9. Mitogen Stimulation of $B6CF_1$ Spleen Cells

Age (days)	Radiation[a]	Response to Mitogen[b]		
		Con A (2 μg/ml)	PHA (2 μg/ml)	LPS (0.2 μg/ml)
100	0	195,313 ± 23,878	52,826 ± 3,878	17,362[c]
160	0	137,625 ± 13,954	56,702 ± 7,503	-
250	0	57,219 ± 9,376	-	-
	855 γ	73,528 ± 6,953	-	-
330	0	95,703 ± 19,951	-	-
415	0	76,354 ± 8,762	31,164 ± 2,996	5,928 ± 2,954
	240 fn	84,908 ± 18,055	59,116 ± 11,244	9,110 ± 1,544

[a]Mice were irradiated at 110 days of age with a single dose of either 240 fn at a dose rate of 17 rad/min or 855 γ at a dose rate of 50 rad/min.

[b]The response is shown as the increase in counts per minute of tritiated thymidine from unstimulated control cultures ± 1 standard error.

[c]Only one determination at this age; 5-10 mice were used at other ages.

CONCLUSIONS

Single doses of 288 neutron rad or 740 gamma rad interfered with the ability of the host to kill a challenge dose of *P. pneumotropica* 5, 11, and 21 days after irradiation. Neutron-irradiated mice showed little repair by 21 days, but some repair was evident in gamma-irradiated mice. The same doses of radiation dramatically depressed the spleen T-cell content. The T-cell content in gamma-irradiated mice returned to normal by 21 days, but that in neutron-irradiated mice did not.

An age-related decline in the response of cultured spleen cells to mitogen stimulation was observed which closely paralleled the decline of Θ antigen previously reported (3).

REFERENCES

1. Ainsworth, E. J., R. J. M. Fry, D. Grahn, F. S. Williamson, P. C. Brennan, S. P. Stearner, A. V. Carrano, and J. H. Rust. In: Biological Effects of Neutron Irradiation IAEA, Austria, 1974, p. 359.
2. Brennan, P. C., and W. T. Kickels. The JANUS Project Semiannual Report No. 5, p. 58 (Jan., 1973).
3. Brennan, P. C., and B. N. Jaroslow. Cell. Immunol. 15, 51 (1975).
4. Brennan, P. C., R. C. Simkins, and R. T. Collins. ANL-8070 (1973), p. 20.

AGE-ASSOCIATED DECLINE IN THETA ANTIGEN ON SPLEEN THYMUS-DERIVED LYMPHOCYTES OF $B6CF_1$ MICE*

Patricia C. Brennan and Bernard N. Jaroslow

The proportion of theta-bearing cells in spleen cell suspensions of normal $B6CF_1$ mice of both sexes, from 1-900 days of age was determined using indirect immunofluorescence. By 25 days of age theta positive cells constituted ∿ 32% of the population and this proportion remained constant to 183 days of age. Between 183 and 650 days of age the proportion of theta positive cells declined linearly. The amount of theta antigen per cell also decreased with age. Theta was visualized as a continuous ring on cells from young mice and changed to a patchy distribution to faintly visible incomplete rings by 600 days of age.

The age-associated decline in theta antigen suggests that the amount of theta on the cell surface is an indicator of, and perhaps a contributor to, the functional capability of the thymus-derived cell.

*Abstract of a paper published in Cellular Immunology 15, 51 (1975).

A UNIQUE AND VERSATILE GAMMA IRRADIATION FACILITY

Frank S. Williamson, Gordon L. Holmblad, Joseph E. Trier, and Emil G. Johnson, Jr.

PURPOSE AND METHODS

Experience with the JM-2 experimental series has emphasized the desirability of a gamma irradiation facility which combines a capacity of at

least 400 mice per exposure with a range of dose rates encompassing at least a factor of 1000.

PROGRESS REPORT

An Atomic Energy of Canada Gammabeam 650 panoramic irradiator has been installed in the High Level Gamma Room and calibrated. As manufactured, this unit has 12 source tubes containing 12 sources which may be exposed in any combination. Furthermore, the pitch-circle diameter of the exposed sources may be adjusted so as to irradiate a central volume at high dose rates with good uniformity.

The unit was ordered with a novel source loading (Cobalt-60). The 12 sources specified were:

5000, 5000, 5000, 5000, 2500, 1250, 625, 320, 160, 80, 40, 20 Curies.

Hence, by using only 1 source we can obtain an intensity in the range 20-5000 Ci, by factors of 2. By using 2 or 4 sources of 5000 Ci the range is similarly extended to 20,000 Ci.

Panoramic Geometry

These combinations add valuable new dimensions but complicate the dosimetry. For example, no single source is ever at the center of the room and it is not feasible to mark the floor with a coordinate grid for each separate source.

A floor grid has been laid out in polar coordinates originating at the center of symmetry of the source system. A computer program has been written to calculate exposure rates from the various sources, allowing for floor scatter. In setting up an irradiation using load frames which hold mouse containers, this information is used to narrow down the zone in which exposure-rate measurements are made. A second program calculates exposure-rate distribution in the load frame, with the mean, and is used to estimate the target exposure rate, at the frame center, that will produce the desired mean. The required orientation of the frame with respect to the floor grid is also computed.

Typical conditions, showing the estimated worst-case deviation from the mean of the exposure to a single mouse, are shown in Table 4.10. A continuously variable exposure rate from 0.04 to 23 R/min is available to irradiate 500 mice in a 10-frame load, with a worst-case deviation from the mean exposure to one mouse of better than 7%.

Central Geometry

The four strongest sources are disposed in tubes so that, when exposed, they are equidistant on the circumference of a circle. In typical geometries (sources in November, 1974):

Sources on 14-cm diam circle - central exposure rate 30,000 R/min.
Sources on 30-cm diam circle - central exposure rate 8960 R/min.

In a volume 8-cm high by 8-cm diameter, the exposure rate is uniform to ± 2%.

Table 4.10. High Level Gamma Room in Panoramic Geometry Source Strength on October 17, 1974

Source Ci	Distance from Source Axis cm	Exposure Rate R/min	No. of Frames	No. of Mice	Maximum Deviation from the Mean %
16.4	300	0.037	10	500	-2.7
16.4	170	0.108	10	500	-6.1
3253	170	22.7	10	500	-6.1
12941[a]	238[b]	45.5	4	200	-3.4

[a]Four sources.

[b]From center of irradiator.

CONCLUSION

This new gamma irradiation facility provides an extremely wide range of exposure rates and will go far toward fulfilling the diverse requirements of this Division for acute and fractionated exposures.

DOSIMETRY OF A π^- BEAM AT THE ZERO GRADIENT SYNCHROTRON

Thomas B. Borak, Gordon L. Holmblad, and Frank S. Williamson

The unique electromagnetic and nuclear properties of the negative pi (π) meson make it a particularly good candidate for use in radiotherapy (1,2). Considerable radiobiological data need to be accumulated, however, before clinical applications can be inaugurated. We, therefore, participated in a particle production survey to determine if existing accelerator facilities at Argonne are adequate for a research program in pion radiobiology.

The experiment was conducted at secondary beam line 42 in the west experimental hall of the Argonne Zero Gradient Synchrotron (ZGS). This beam was designed to transport 200 MeV/c charged particles every ZGS pulse. Pilot-B plastic scintillation detectors were placed at several locations downstream of the momentum selection slit. The distance between the first and last paired coincidence counters was sufficient to allow for time of flight separation of light particles (electrons) and heavy particles (pions and muons).

Due to the pulsed nature of the beam and uncertainties in intensity, dosimetry measurements were made with a small (1.0 cm x 1.0 cm x 0.32 cm) plastic scintillator. This detector was placed at a focal point about 40 cm downstream from the last quadropole doublet, and was surrounded by a movable

water phantom. The light emitted when a charged particle passes through or interacts in the detector was sampled by a photomultiplier tube. The output was amplified and transferred into a 512 channel pulse height analyzer gated by the time of flight system.

Figure 4.4 shows several energy deposition spectra as a function of depth. Note that at zero depth both pions and muons are minimum ionizing, and therefore indistinguishable. At greater depths the pions begin losing energy more rapidly than do the muons and the resulting heavier ionization is characterized by a progressive shift toward higher energy deposition. Finally near the end of the pion range the high LET nuclear fragments deposit large amounts of energy, whereas the muons are just beginning to slow down. The small shoulder at low energies is produced by minimum ionizing electrons.

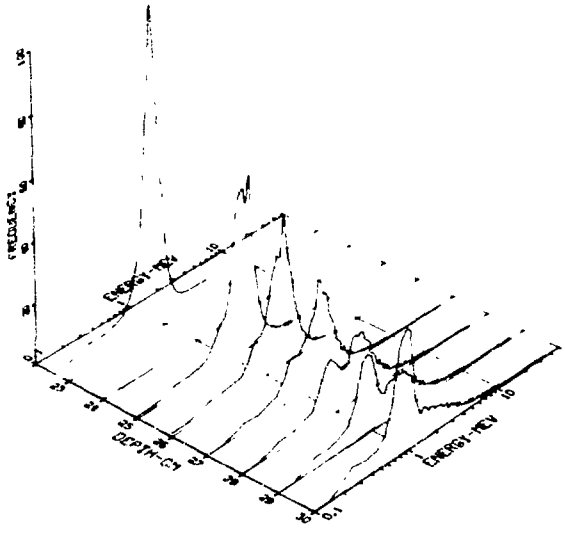

Fig. 4.4. Differential energy-deposition spectra of 200 MeV negative pions at various depths in a water phantom.

These differential energy spectra can be integrated to yield absorbed dose in the plastic as a function of depth in the phantom. Figure 4.5 shows the relative depth dose properties observed in this experiment. The characteristic peak at the pion end of range is clearly evident. However, the slope of the "plateau" region is much steeper than reported elsewhere (3,4).

A calculation incorporating multiple Coulomb scattering (MCS) and nuclear collisions was made to aid in interpreting the observed slope. We assumed a parallel beam with intensities weighted by transverse beam profile measurements. MCS was incorporated in the form of an energy dependent gaussian with ionization energy loss according to the work of Sternheimer (5,6). A polynomial fit was used for the nuclear scattering cross section, noting that the incident energy (104 MeV) lies within the P_{33} π-nucleon resonance region (7).

The results of this calculation, shown by the dashed curve in Figure 4.5, are in excellent agreement with a Monte Carlo computation also using a parallel beam (8). The divergence between the calculated and measured data

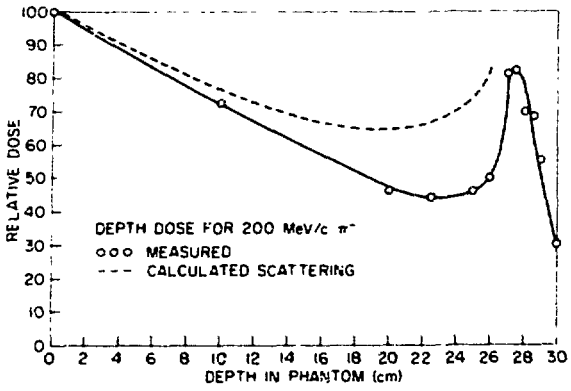

Fig. 4.5. Measured and calculated depth dose distributions for 200 MeV negative pions.

suggests that the greater slope may be caused by the large geometrical fluctuations of the beam at the focal point of the magnetic lens.

Using the measured values of absolute intensity per pulse and a duty cycle of 1 pulse every 4.6 seconds, we arrived at a dose rate in the stopping region of 1.2 ± 0.3 mrad/min. Attempts to measure the dose with ionization chambers were unsuccessful because of the extremely small signals produced by this beam intensity.

CONCLUSIONS

The dose rate of 1.2 mrad/min is several orders of magnitude below that convenient for radiobiological experiments. This could be increased by a factor of 4 by increasing the external proton current on the beam 42 production target. The secondary particle contamination in a 100 MeV pion beam produced from a 12 GeV source deserves strict attention. Reliability and tolerance levels of all beam components must be carefully scrutinized since biological specimens, as opposed to fast electronics, cannot "gate-off" after each beam separator failure.

ACKNOWLEDGMENT

We wish to acknowledge the cooperation of the Argonne Accelerator Facilities Division.

REFERENCES

1. Fowler, P. H., and D. H. Perkins. Nature (London) 180, 524 (1961).
2. Fowler, P. H. Proc. Phys. Soc. (London) 85, 105 (1965).
3. Sullivan, A. H., and J. Baarli. CERN Rep. DI/HP/148 (1972).
4. Duerrannois, J. R., R. N. Hamm, J. E. Turner, and H. A. Wright. Phys. Med. Biol. 17, 765 (1972).
5. Sternheimer, R. M. Phys. Rev. 91, 256 (1953).
6. Sternheimer, R. M. Phys. Rev. 103, 511 (1956).
7. Lock, W. O., and D. F. Meadsay. Intermediate Energy Nuclear Phys, Metheun, London, 1970.
8. Wright, H. A. Oak Ridge National Laboratory. Personal communication (1974).

A QUALITY CONTROL TECHNIQUE FOR GEOMETRICAL REPRESENTATIONS IN THE BIM-130 MONTE CARLO TRANSPORT CODE

Thomas B. Borak

PURPOSE AND METHODS

The BIM dosimetry group maintains a large Monte Carlo neutron-gamma ray transport code titled BIM-130 (1). This code is used to compliment and in some instances supplement physical measurements. It has the capacity to trace the intersection and scattering of particles through 45 geometric regions, each of which has a chemical composition containing up to 15 elements.

The 45 regions are mathematically defined in the program through a three-dimensional Cartesian coordinate system. The boundaries are prescribed by input data containing the central location and orthogonal half widths. With this type of arrangement there is always a problem of quality control; mainly, is the information on the data cards correctly converted into the true geometrical pattern of interest within the program? A small error could be drastic and expensive!

We have developed a test code to check and confirm the shapes of the regions described by the input data. The program, called BIMBOX, uses the actual portion of the Monte Carlo code which makes geometrical decisions. To this is coupled an arsenal of idealized particle sources which can be aimed with chosen directions and locations. The intersections of these particles with respective regions is scored and stored in appropriate arrays. These arrays are then displayed in the form of printer plots and if desired on a Calcomp plotter using the ANL DISSPLA package.

Figure 4.6 shows the configuration of an irradiation room (15.5 x 5.0 m^2) filled with nested cylinders whose axes of rotation are parallel to the Z direction. The central region is reduced to a straight line, but can be magnified by using the ZOOM characteristics of the program.

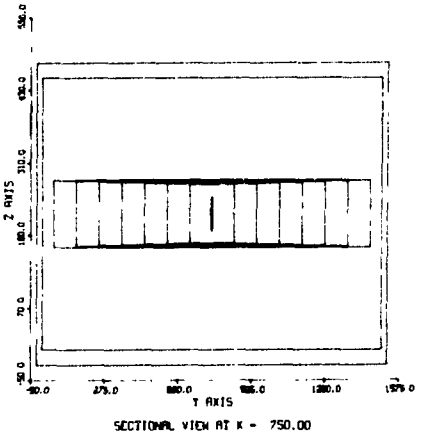

Fig. 4.6. Elevation view of an irradiation facility filled with concentric cylinders. The vertical line in the center contains the ^{60}Co source.

Figures 4.7 and 4.8 show two magnified views of the central region which represents the capsulated ^{60}Co source in an AECL Gamma Beam 150.

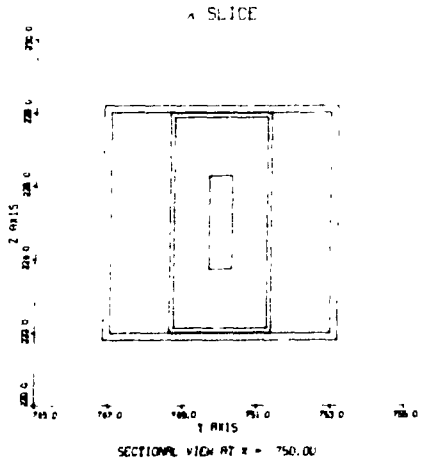

Fig. 4.7. Magnified elevation view of the ^{60}Co source and container shown in Figure 4.6.

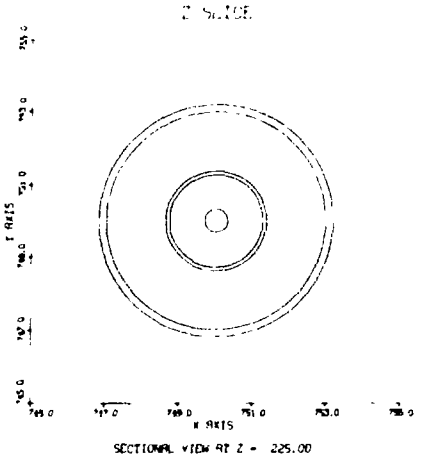

Fig. 4.8. Plan view of the ^{60}Co source and container shown in Figure 4.7.

The correct nesting sequence can be confirmed in the printer plots where the boundaries of each region are identified with coded characters. Execution for this example of 16 regions was performed within 250 K bytes of core in less than 30 seconds on an IBM 370/195.

REFERENCE

1. Frigerio, N. A., R. F. Coley, and M. H. Branson. Phys. Med. Biol. 18, 53 (1973).

A SIMPLE APPROACH TO CALCULATING GAMMA RAY SKYSHINE FOR REDUCED SHIELDING APPLICATIONS

Thomas B. Borak

PURPOSE AND METHODS

New irradiation facilities at ANL (1) and elsewhere are being designed with the minimum radiation shielding. Usually the first victim of these austerity measures is the roof. This increases the amount of radiation escaping skyward and atmospherically reflected toward neighboring facilities. Below we present a simplified single scatter treatment of SKYSHINE. The pessimistic case with forward shielding wall and source reduces to a single summation which can be performed on a desk calculator.

Given a monoenergetic isotropic source of gamma rays, the intensity of singly scattered photons at distance X can be represented by (see Figure 4.9):

$$I = \frac{SN}{4\pi X} \int_{\psi_o}^{\pi-\phi_o} d\psi \int_{\phi_o}^{\pi-\psi} d\phi \int_{0}^{A_z} dAz \; \frac{d\sigma}{d\Omega}(\theta = \psi + \phi) \qquad (1)$$

where

S = photons/second emitted by source
N = number of electrons/cm^3 in air
$\frac{d\sigma}{d\Omega}(\theta)$ = differential Compton scattering cross section (cm^2/electron)
A_z = Azimuthal acceptance of scattering volume
X = distance from source to detector in cm.

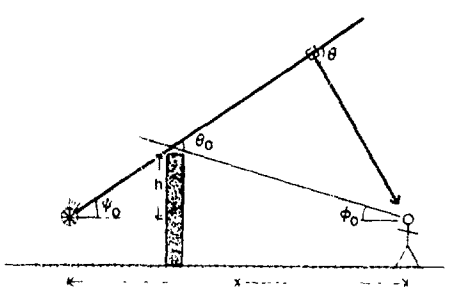

Fig. 4.9. Schematic diagram illustrating the symbols and angles defined by equations 1-5. The wall in all cases is perpendicular to the vector along X, with effective height above source equal to h.

For the pessimistic case of full hemispherical scattering volume ($A_Z = \pi$), the elevation of the shielding wall reduces to a semicircle of radius h. The photon energy scattered into the detector at X is:

$$I_E = \frac{E_\gamma SN}{4X} \Delta\theta^2 \sum_{\theta = \psi_o + \phi_o}^{179} (\theta + 1 - \psi_o - \phi_o) \frac{d\sigma_E}{d\Omega}(\theta) \qquad (2)$$

Here the sum is carried over integral degree values but the differential increment remains in radians ($\Delta\theta = 0.0175$). All energy units are in MeV. The energy scattered Compton formula can be obtained graphically (2) or calculated:

$$\frac{d\sigma_E}{d\Omega} = 3.97 \times 10^{-26} [F^2 + F^4 - F^3 \sin^2 \theta] \qquad (3)$$

$$F = \frac{E}{E_\gamma} = [1 + \frac{E_\gamma}{.511} (1 - \cos \theta)]^{-1} \qquad (4)$$

Realistically the azimuthal acceptance is limited by the size of the forward wall or side walls. For the case of a semi-infinite wall of height h, the limits of integration depend on ψ, but can easily be incorporated yielding:

$$I_E = \frac{E_\gamma SN}{4\pi X} \int_{\psi_o}^{180-\phi_o} d\psi \int_{\phi_o}^{180-\psi} d\phi \; 2 \cos^{-1} \left(\frac{h \sin (\psi + \phi)}{X \sin (\psi) \sin (\phi)} \right) \frac{d\sigma_E}{d\Omega} (\psi + \phi) \qquad (5)$$

where now a double sum must be performed.

The dose rate can be obtained by multiplying the results by the appropriate first collision flux to dose conversion factors. Although complex in appearance these sums can easily be made and dose rates rapidly calculated to obtain the potential hazard at various locations outside of the structure.

REFERENCES

1. Norris, W. P., Argonne National Laboratory. Personal communication (1974).
2. Segré. E. Nuclei and Particles, W. A. Benjamin Inc., New York, 1964, p. 55.